Janus PVDF Membrane with Extremely Opposite Wetting Surfaces via One Single Step Unidirectional Segregation Strategy

Journal:	*ACS Applied Materials & Interfaces*
Manuscript ID	am-2018-08278e.R1
Manuscript Type:	Article
Date Submitted by the Author:	n/a
Complete List of Authors:	Li, Tiantian; Ningbo Institute of Materials Technology & Engineering Liu, Fu; Ningbo Institute of Materials Technology and Engineering, Zhang, Shaofei; State Key Laboratory of Separation Membrane and Membrane Processes Lin, Haibo; Ningbo Institute of Materials Technology and Engineering, Chinese Academy of Sciences Wang, Jianqiang; Ningbo Institute of Materials Technology and Engineering Chinese Academy of Sciences, Tang, Chuyang; The University of Hongkong, Hong Kong., Department of Civil Engineering,

Janus PVDF Membrane with Extremely Opposite Wetting Surfaces via One Single Step Unidirectional Segregation Strategy

Tiantian Li[a,b], Fu Liu[a,b]*, Shaofei Zhang[c], Haibo Lin[a], Jianqiang Wang[a,b], Chuyang Y. Tang[d]

a: Key laboratory of Marine Materials and Related Technologies, Ningbo Institute of Materials Technology & Engineering, Chinese Academy of Sciences, No. 1219 Zhongguan West Rd, Ningbo, 315201, China

b: University of Chinese Academy of Sciences, 19 A Yuquan Rd, Shijingshan District, Beijing, 100049, China

c: State Key Laboratory of Separation Membrane and Membrane Processes, School of Materials Science and Engineering, Tianjin Polytechnic University, Tianjin, 300387, China

d: Department of Civil Engineering, The University of Hong Kong, Pokfulam, Hong Kong, China

*Please address correspondences to:

Prof. Fu Liu

Address: Ningbo Institute of Materials Technology & Engineering, Chinese Academy of Sciences, No. 1219 Zhongguan West Rd, Ningbo, 315201, China

Tel.: +8657486325963;

Fax: +8657486325963;

E-mail: fu.liu@nimte.ac.cn

Abstract

Janus membrane with asymmetric wettability has attracted intense attention in oil/water separation, membrane distillation, liquid/fog collection and liquid diode etc. Facile manipulation of paradoxical wetting/anti-wetting property on opposite surfaces of 2D membrane is challenging. Different from most post-modification methods, herein we propose one single step unidirectional segregation strategy to fabricate a polymeric Janus membrane with extremely opposite wetting surfaces showing almost 150 degree contact angle difference for the first time. We achieved the unidirectional segregation of hydrophilic copolymer poly(vinylpyrrolidone-vinyltriethoxysilane) (PVP-VTES) in polyvinylidene fluoride (PVDF) membrane during phase separation. A glycerol coating on the non-woven fabric support locally limited the phase separation on the bottom surface and blocked the segregation of hydrophilic copolymer, and promoted the segregation to the top surface. Working collaboratively with the asymmetric micro-/nano-structure on both surfaces, the resulted Janus membrane exhibited superhydrophilic top surface and superhydrophobic bottom surface. Janus PVDF membrane showed switchable separation performance and high separation efficiency for both oil-in-water emulsion and water-in-oil emulsion due to the anisotropic wettability compared with solely hydrophobic or hydrophilic PVDF membranes.

Keywords: Janus membrane, unidirectional segregation, emulsion separation, PVDF membrane, phase inversion

1. Introduction

The term Janus was first introduced by De Gennes to describe particles with different hemispheres from a chemical point of view in 1991.[1] Janus is the god in ancient Roman religion and myth depicted as having two faces, one side looking to the future and the other side looking to the past. Therefore, materials with asymmetric structures or properties are named as Janus materials, including Janus particles,[2-4] Janus nanosheets[5, 6] and Janus membranes.[7-10] Among these materials, Janus

membranes have attracted great attention due to their asymmetric wettability. The directional liquid transportation was mostly investigated by virtue of Laplace pressure (ΔP) of Janus membrane. A Janus membrane originated from polyethylene terephthalate (PET)/polytetrafluoroethylene (PTFE) composite porous membrane could realize the smart application in water collection, lossless transportation, decontamination, and on-off control.[11, 12] It should be noted that the hydrophobic surface possessed big enough pores and thin enough thickness for the water droplet transportation. Janus cotton fabric with side length reaching 200 μm realized the coalescence of micrometer-sized oil droplets and transportation while repelling water by both hydrophobic side and oil filled side.[13-15] Different from the demulsification separation, the direct exclusion separation based on pore size could also be achieved by PAN/CNTs membrane.[16] Hydrophobic CNTs was deposited on the hydrophilic PAN electrospinning membrane to form the Janus membrane. Janus hollow fiber membrane can also be prepared by the lumen coating of PDA/PEI layer, which was used to promote high mass transfer in conventional direct contact membrane distillation (DCMD).[17] Other intriguing applications were explored in fine bubble production,[18] emulsion production,[9] fog collection.[19]

The preparation of above macroporous materials (e.g. 200 μm cotton fiber) is usually involved with the post-modification with pre-synthesized polymer, which is costly and low efficient. It is challenging to construct Janus polymeric membranes via one single step. Up to now, most of Janus membrane fabrication can be considered as a post-modification strategy including surface coating,[18, 20] surface grafting,[13, 21] electro-spinning[22, 23] and vaporization induced phase inversion.[24, 25] For example, PP membrane was floated on DA/PEI solution surface to adhere hydrophilic PDA/PEI coating through a "down-top" way.[18] The "top-down" method was commonly used to coat a polymeric layer on substrate for different wettability.[20] This method required the coating solution with higher viscosity to avoid its diffusion from one side to other side due to the capillary effect, affecting the asymmetric wettability. Electrospinning was also used to fabricate Janus membrane. The hydrophobic polyurethane (PU) and hydrophilic crosslinked poly(vinyl alcohol) (c-PVA) nanofibrous composite

membrane was prepared by sequential electrospinning.[23] However, so prepared Janus membrane by electrospinning lacked the strong bonding interaction between PU and c-PVA. Traditional phase inversion can be used to prepare porous membrane.[26] Vaporization induced phase inversion was used to fabricate Janus membrane. M. Essalhi et al firstly synthesized fluorinated surface modifying macromolecule (SMM) and then blended it with PEI solution.[24] The casting solution was wiped on a glass plate, remaining 30 seconds in ambient temperature to let SMM migrate to the polymer/air interface. Zhang et al found that different solvents can affect the migration of dynamic frameworks and the asymmetric wettability between two sides can reach to the maximum when CH_3CN was used as solvent.[25] However, it's a long way to go to achieve the real Janus membrane with extremely opposite wettability on both sides with the contact angle difference up to 150 degree. The conventional non-solvent induced phase separation is challenging to obtain Janus membrane with opposite properties. The reason is that the migration of functional additives in the polymer matrix is usually isotropic to achieve the lowest surface tension. The water environment will induce the hydrophilic components migrate to both top and bottom surfaces. Therefore, the resulted membrane has similar properties in terms of top and bottom surfaces, which cannot be considered to be a real Janus membrane. Previous studies showed that the physical morphology and chemical composition anisotropy was constructed sequentially or independently. Multi-steps were necessary to obtain the above Janus properties.

Distinctly from above studies, we aim to develop Janus PVDF membrane with extremely opposite wetting surfaces via one single step unidirectional segregation strategy. The water contact angle difference between two sides is up to 150^o, which outnumbers all previous results. We introduced a glycerol sacrificial coating on the non-woven fabric support to control the one-way migration of hydrophilic copolymer PVP-VTES during phase inversion. PVP-VTES was solely migrated onto the top from the inside polymeric solution to form a superhydrophilic surface. The glycerol coating blocked the exchange between coagulation bath and solvent in casting solution and limited the phase separation on the bottom surface and therefore repelled

the segregation of hydrophilic compolymer. Working collaboratively with micro-/nano-structure imprinted from non-woven fabric support, the bottom surface exhibited superhydrophobic property with the contact angle up to 150 degree. The hydrolytic crosslinking of silane coupling agent of PVP-VTES in the subsequent heat treatment process fixed the hydrophilic polymer on the top surface firmly. The controllable unidirectional migration path of hydrophilic polymer in PVDF membrane can be considered as an "inside-out" segregation, PVP-VTES migrates to the outside coagulation bath from inside the solution. Janus PVDF membrane showed excellent separation performances for both oil-in-water and water-in-oil emulsions in contrast to the solely superhydrophobic or superhydrophilic membrane.

2. Experimental section

2.1 Materials

Triethyl phosphate (TEP), Vinyltriethoxysilane (VTES), Trichloromethane ($CHCl_3$), toluene, Span 80 and glycerol were provided by Sinopharm Chemical Reagent Co. Ltd., China. 1-Vinyl-2-pyrrolidone (NVP, 99%) and 2, 2'-Azobis (2-methyl propionitrile) (AIBN, 99%) were purchased from Shanghai Aladdin Chemistry Co. Ltd., China. Polyvinylidene fluoride (PVDF) (Kynar 761-A, Arkema) was dried at 60 ^{o}C before use.

2.2 Fabrication of PVDF membrane with opposite wettability

15.0 g PVDF was dissolved in 85.0 g TEP at 80 ^{o}C and stirred at 300 r speed for 3 hours under nitrogen atmosphere. After PVDF was completely dissolved, 3.75 g NVP, 2.75 g VTES and 0.08 g AIBN were quickly added into dissolved PVDF solution. The "*in-situ*" polymerization was carried out at 80 ^{o}C with 500 r stirring under nitrogen atmosphere for 24 hours. The solution was deaerated under reduced pressure and then kept at 80 ^{o}C for 6 hours without stirring to remove residual bubbles.

The non-woven fabric (PET, 90 g/m^2) was immersed in glycerol for certain time. The excess glycerol on non-woven fabric was absorbed by filter paper to allow the casting solution to spread smoothly on the non-woven fabric. The glycerol content on

the non-woven fabric was tuned by ratio of glycerol to water (v/v). After the non-woven fabric was dried at 50 ^{o}C for 2 hours, the water in non-woven fabrics was evaporated and glycerol remained due to the different boiling point of glycerol (290.9 ^{o}C) and water (100 ^{o}C). Lastly, casting solution mentioned-above was casted on the glycerol-coated non-woven fabric support using casting knife with a gap of 200 μm. The nascent membrane was immediately immersed into a bath composed of TEP/water mixture (v/v: 5/5) for 5 seconds, and then transferred to fresh deionized water at 60 ^{o}C for 24 h to complete membrane solidification and PVP-VTES cross-linking. Afterwards, the membranes were transferred to fresh deionized water at ambient temperature for 48 h to remove the residual solvent and glycerol. The membranes were dried out in air and peeled off from non-woven fabric for further experiment. The new surface generated from peeling was defined as bottom surface and the opposite side was top surface accordingly. PVDF Janus membrane was named as M2, M3 and M4 respectively according to the ratio of glycerol/water as listed in **Table 1** (v/v: 3/7, 5/5 and 1/0 respectively).

In contrast, the hydrophilic PVDF membrane and hydrophobic PVDF membrane with symmetrical wettability were also fabricated. For hydrophobic PVDF membrane named as M1, the "*in-situ"* polymerization of PVP-VTES was not involved. The casting solution with 15.0 g PVDF and 85.0 g TEP was scraped on non-woven fabrics by casting knife with gap of 200 μm. Then the liquid membranes were also immersed in coagulation bath as mentioned above (TEP/water) for 5 seconds and transferred to deionized water to remove residual solvent. For hydrophilic PVDF membrane named as M5, the non-woven fabrics was not dealt with glycerol. And the casting solution composition and casting procedure were implemented in accordance with above experiments.

Table 1. Hydrophobic M1, Janus M2-M4 and hydrophilic M5 membranes.

Code	M1	M2	M3	M4	M5
Oil	---	Gly/Water (v/v: 3/7)	Gly/Water (v/v: 5/5)	Gly	---

* The non-woven fabrics for M1 and M5 aren't dealt with glycerol.

2.3 Membrane characterization

Field emission scanning electron microscope (S4800, Hitachi, Japan) was used to analyze the morphology of membrane. The wettability for top surface and bottom surface were detected using contact angle meter (OCA20, Dataphysics, Germany) and five measurements were recorded at different positions. The molecular weight of PVP-VTES was measured using gel permeation chromatography (PL-GPC 220, China). The element compositions of both sides were measured by X-ray photoelectron spectroscopy with Mg-Kα as radiation resource (XPS, Shimadzu Axis Utltradld spectroscope, Japan) and attenuated total reflectance fourier transform infrared spectra (ATR-FTIR, Thermo-Nicolet 6700, US). 3D roughness images of the membrane and the thickness of hydrophilic layer were recorded by laser scanning confocal microscope (LSM700, Zeiss, Germany). The purities of the feeds and filtrates for water-in-oil emulsion and oil-in-water emulsion were analyzed by Karl Fischer Titrator (Mettler Toledo DL31, Switzerland) and total organic carbon analyzer (TOC, multi N/C2100, analytikjena, Germany), respectively.

2.4 Preparation and separation of oil-in-water and water-in-oil emulsions

For oil-in-water emulsion, 1mL trichloromethane was added into 99 mL deionized water and stirred vigorously for 24 hours. For water-in-oil emulsion, 0.8 mL deionized water and 80 mL toluene were stirred under 600 r speed in the presence of 0.25 g Span 80 (HLB = 4.3). The separation processes were manipulated by vacuum driven filtration system at -0.09 MPa and each sample was tested three times. The flux and rejection for emulsions were calculated using following equation (1) and equation (2), respectively.

$$Flux = \frac{V}{S \times t} \qquad (1)$$

$$R = \left(1 - \frac{P_{filtrate}}{P_{feed}}\right) \times 100\% \qquad (2)$$

where V (L) is the volume of filtrate; S (12.56×10^{-4} m^2) is the effective area of

membranes; t is the testing time; $P_{filtrate}$ and P_{feed} are the purities of the filtrates and feeds, respectively.

3. Results and discussion

3.1 Opposite wettability of Janus PVDF membranes

As listed in **Table 1**, Janus membranes were named as M2, M3 and M4 according to the different ratio of glycerol/water on the non-woven fabric support, respectively, while the hydrophobic and hydrophilic membrane were named as M1 and M5. The effects of different oils including silicone oil, soybean oil and liquid paraffin on the experimental results were also studied in details (**Table S1**). It is noted that the oil chosen in this experiment has relatively low viscosity for easily coating on non-woven fabric.

The water contact angles (WCA) of the membranes in air were measured for both top and bottom surfaces. Janus PVDF membranes (M2, M3 and M4) showed distinctly opposite wetting behaviour for both surfaces. As shown in **Figure 1a**, **1b** and **1c**, the top surface of M2, M3 and M4 showed instantaneous wettability. The contact angle decreased to 0 in less than 2 seconds and the water droplet spread on the surface, forming a wathet blue circle. The superhydrophilicity was mainly ascribed to the high enrichment of crosslinked PVP-VTES. While the bottom surface exhibited high hydrophobicity. The water contact angle is 115^o, 130^o and 140^o for M2, M3 and M4 respectively. And the spherical wathet blue water droplet stands on the bottom surface without staining the membrane. Furthermore, with increasing the glycerol content on the non-woven fabrics, the bottom surface displayed enhanced hydrophobicity. Similarly, when the non-woven fabric was coated with silicone oil, soybean oil and liquid paraffin respectively, the as-prepared membrane N1, N2 and N3 also showed superhydrophilic top surface and superhydrophobic bottom surface. Contact angle differences between both surfaces can reach ~140^o, as shown in **Figure S1**. In contrast, M1 membrane showed high hydrophobicity for both top and bottom surfaces, and the water contact angles in air for top and bottom surfaces were 110^o and 149^o, respectively. M5 membrane showed instantaneous wettability for both top

and bottom surfaces. Therefore, Janus PVDF membrane demonstrated tremendously opposite wetting behaviour. The contact angle differences ($\Delta\theta\approx140^{o}$) between top and bottom surfaces are generally higher than previously reported results, as listed in **Table 2**. Therefore, the paradoxical wetting/anti-wetting property was achieved on PVDF membrane via the single step unidirectional segregation strategy, which is more convenient and efficient than the previous post-modification methods such as surface coating, surface grafting and electrospinning. The porous superhydrophilic top surface is mainly governed by the enrichment of hydrophilic PVP-VTES, and the bottom surface shows a superhydrophobic Cassie state, as illustrated in **Figure 1c**. The multi-scaled micro-/nano-structure was produced from the phase separation, crystallization and peeling from non-woven fabrics. The textured surface containing air cushion repelled the pinning and intrusion of water droplet. More importantly, the glycerol with higher viscosity than water coating on the non-woven fabrics prevented quick intrusion of non-solvent water from the bottom surface, and PVP-VTES was limited to segregate to the bottom surface during phase separation. It was easily dragged to the top surface directly contacting with water due to its hydrophilicity and lower molecular weight (M_w=2197). Therefore, the sacrificial oil coating (glycerol, silicone oil, soybean oil and liquid paraffin) resulted in the unidirectional migration and asymmetric distribution of PVP-VTES across the membrane.

From **Figure 1c**, we can observe that the bottom surface site of Janus membrane (M2, M3 and M4) kept dry and hydrophobic even though the water droplet intruded and wetted the corresponding opposite site on top surface. It is indicated that the water droplet was hindered on the interface between hydrophilic and hydrophobic layer. In comparison, no interface was found in the hydrophobic membrane M1 and hydrophilic membrane M5, demonstrating same wetting behavior for both sides. For M1, the low surface energy PVDF component contributed to the hydrophobic surface and the coarser texture resulted the superhydrophobicity (149^{o}). For M5, the absence of oil coating on non-woven fabric caused the same water exchange behavior for both sides, and the hydrophilic copolymer was able to segregate to both surfaces in an isotropic way, which resulted in superhydrophilic top and bottom surfaces.

The hydrophobic/hydrophilic stability of M4 membrane was further investigated. PVP-VTES before crosslinking is easily dissolved in ethanol and even the ethanol can be used as solvent to fabricate PVP-VTES. However, it is difficult to be dissolved into ethanol after crosslinking due to the forming of networks through Si-O-Si bonds. Therefore, membrane M4 was immersed into ethanol for one week and then dried in air to measure the water contact angle in order to investigate its stability after crosslinking. The top surface exhibited excellent wettability and the bottom surface kept high contact angle around 140^{o}, as shown in **Figure 2**. The crosslinked PVP-VTES on the membrane top surface was firmly anchored and failed to elute even the membrane was swelled by ethanol.

Table 2. Comparison of the asymmetric wettability of this study with other works.

Method	Contact angle (θ_1, ^{o})	Contact angle (θ_2, ^{o})	$\Delta\theta$ (θ_1-θ_2,^{o})	Ref.
Coating PDA and PEI on PP surface	~110	~0	~110	18
Surface coating	~140	~40	~100	27
Surface grafting	~150	~17	~133	21
Polydopamine-coated SWCNT/SWCNT bilayer membranes	~104	~48	~56	28
Template partial phase segregation	~86.2	~0	~86.2	25
Surface segregation of fluorinated modifying macromolecule	94.4 ± 0.7	78.6 ± 0.6	~15.8	24
Co-extrusion (Hollow fiber)	~140	~50	~90	29
Combination of wet casting and electro-spinning	142.9 ± 1.3	21.5 ± 4.8	~120	22
Electro-spinning	142.2 ± 1.5	22.1±1.3	~120	23
Peeling off the top skin layer of PET/PTFE@TA-DETA using an adhesive tape	~115	~16	~99	11
Unidirectional surface migration	~140	~0	~140	This study

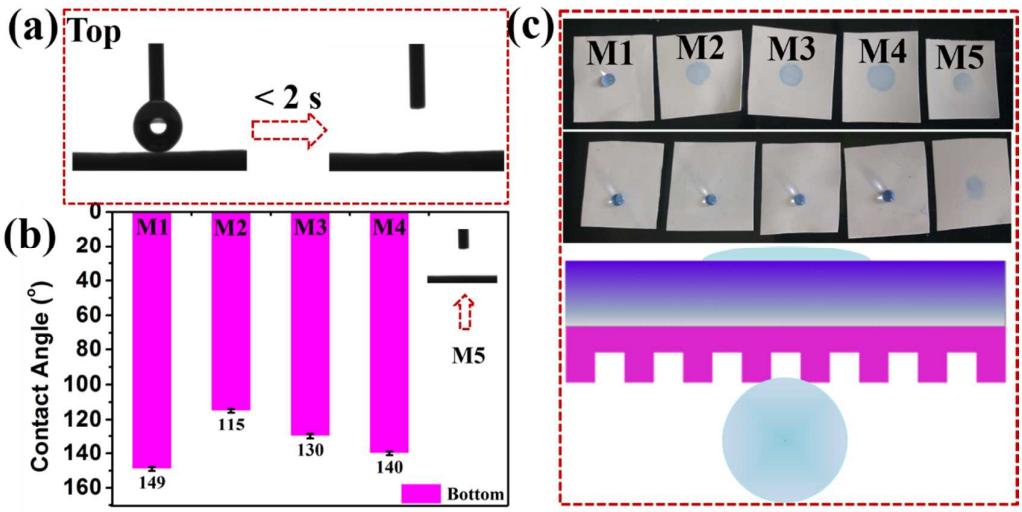

Figure 1. (a) Water contact angles of top surfaces (M2-M5). The water contact angle of top surface for M1 was 110°. (b) Water contact angles of bottom surfaces (M1-M5). The insert in (b) indicated that the water contact angle for M5 was 0°. (c) The images of water droplets (dyed with vitoria blue) on the surfaces of membranes and schematic diagram of water droplets on Janus membrane surfaces. The water volume was 2 μL.

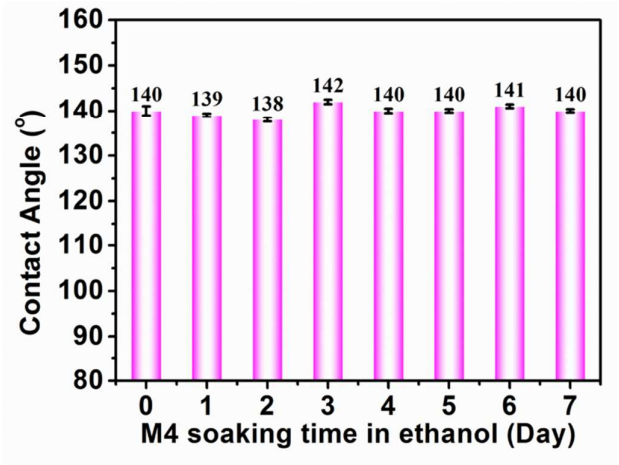

Figure 2. The water contact angle of bottom surface for M4 after the membrane was soaked in ethanol for different days.

3.2 Surface topography and chemistry of Janus membranes

The membrane surface wettability was governed by chemical compositions and topographies.[11, 22] The surface with low surface energy elements and micro/nano-structure tends to be superhydrophobic. On the contrary, the surface with

high surface energy elements and micro/nano-structure tends to be superhydrophilic. From **Figure 3**, we can see that the bottom surfaces for Janus membrane M2, M3 and M4 showed abundent multiscale structures consisting of grooves from donzes to hundreds micrometers, macro-/micro-/nano-pores and spherulites, which was caused by the peeling from non-woven fabrics, phase separation and crystallination of PVDF membranes. 3D confocal microscope images showed that the roughness for M2, M3 and M4 was 12.24, 13.52 and 11.37 μm, respectively. M1, M5, N1, N2 and N3 showed the similar texture and high roughness as showed in **Figure S2** and **Figure S3**. For M1, the bottom surface exhibited sharp peaks, which was probably caused by the tight hydrophobic-hydrophobic interaction. It is more difficult to peel M1 from the non-woven fabric support. For the top surfaces, all membranes demonstrated quite smooth but porous structures in **Figure S4**. Nevertheless, slight difference can still be found. M2, M3, M4 and N1, N2, N3 showed more porous surface. The unidirectional migration caused rapid water/solvent exchange and also decreased the PVDF concentration in the surface, which is facilitated to the spontaneous phase separation. The cross-seciton demonstrated a gradient evolution structure from spherical crystallines dominated bottom to tight top surface in **Figure S5**. Overall, all Janus membranes exhibited asymmetric morphological structure, and the unidirectional segregation induced by the sacrificial oil coating did not substantially influence the surface and bulk morphology.

Besides the surface topography, the asymmetric surface chemistry was significantly manipulated by the unidirectional segregation, which was characterized by ATR-FTIR and XPS. As shown in **Figure 4** and **Figure S6**, the peak at 1636 cm^{-1} of all membranes disappeared, indicating the absence of monomer with C=C bond and the completion of polymerization and crosslinking. All membranes for both surfaces showed peak at 1656 cm^{-1} and peak at 1291 cm^{-1} ascribed to C=O stretching vibration in PVP-VTES and C-F stretching vibration in PVDF, respectively. The intensity of peak at 1656 cm^{-1} for top surface was higher than that for bottom surface, implying that the PVP-VTES intended to enrich on the top surface. The top surface exhibited a significantly higher O (9.84%), N (3.72%) and Si (2.6%) content than that

(5.5, 2.24 and 1.72%) of bottom surface respectively. For the bottom surface, the intensity of C-F stretching vibration at 1291 cm^{-1} is higher than that of the top surface. The bottom surface of M4 has a higher F content (37.23%) than that of top surface (25.61%).

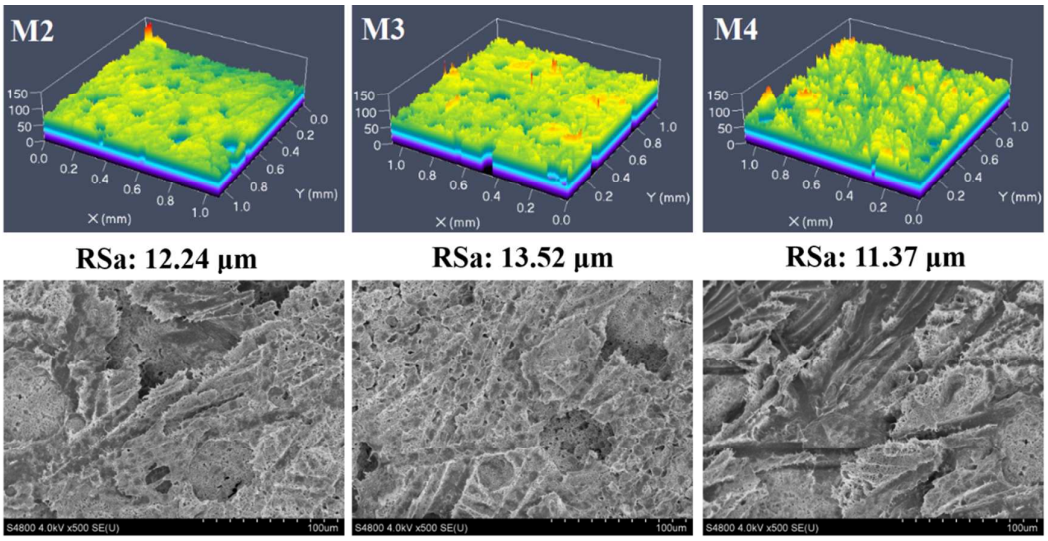

Figure 3. 3D confocal microscope images and SEM images of bottom surfaces of M2, M3 and M4.

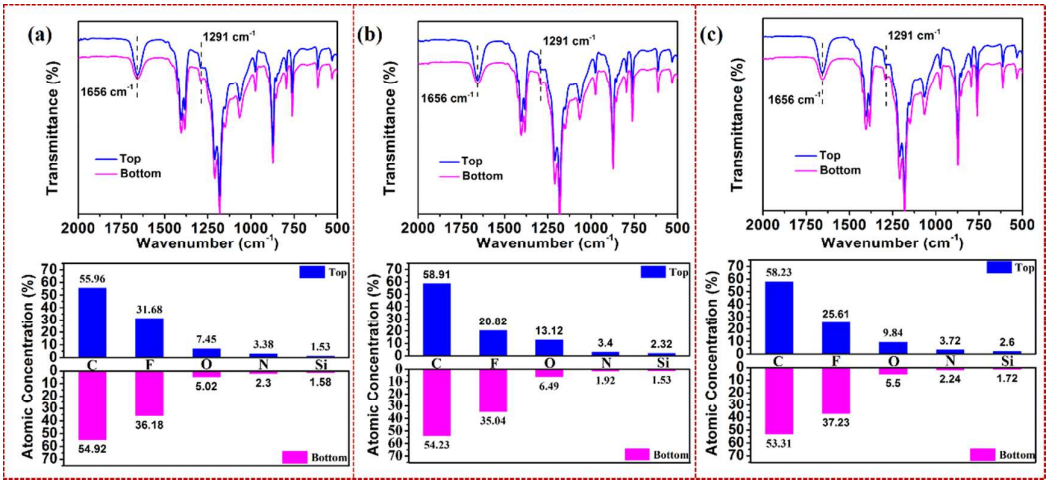

Figure 4. ATR-FTIR and XPS of both surfaces for membrane M2 (a), membrane M3 (b) and membrane M4 (c).

3.3 Unidirectional segregation mechanism

As mentioned above, the hydrophilic copolymer PVP-VTES in membrane was

segregated to the top surface unidirectionally, while the oil coating on the non-woven fabric support hindered its migration to bottom surface due to lower miscibility or insolubility of oil and coagulation bath. The unidirectional segregation mechanism was proposed in **Figure 5**. The water proof glycerol coating switched off solvent/coagulation bath exchange and blocked the coagulation bath intrusion pathway. The phase separation was delayed and limited. While the exchange between coagulation bath and solvent in casting solution only occurred on the top surface contacting with coagulation bath as exhibited in **Figure 5a**. Therefore, the hydrophilic copolymer escaped from the bottom surface and migrated to the top surface to acquire the lower interfacial free energy. The one-way migration was dominated by limited phase separation and surface tension, and caused anisotropy distribution of hydrophilic copolymers from the bottom to the top. After the further hydrothermal cross-linking among VTES segments, the hydrophilic network was fixed firmly inside the membrane in **Figure 5b**. The red crosslinking sites demonstrated the gradient distribution of crosslinking network in the cross-section. After the non-woven fabrics were peeled off, the heterogeneous micro/nano-structure worked with gradient chemical distribution to result in the superhydrophobic bottom surface and superhydrophilic top surface as depicted in **Figure 5c**. The superhydrophobicity was ascribed to the air entrapped into micro/nano-structure resulting in "Cassie-Baxter" synergic effect at air/water/membrane interface, and the water contact angle can be illustrated by equation (3).[30]

$$\cos\theta^* = f(R_f \cos\theta + 1) - 1 \qquad (3)$$

where θ* is the static water contact angle, θ is water contact angle on a flat surface, f is the effective surface area of membrane-water interface and R_f is the factor of surface roughness. Therefore, the low surface energy fluorine enriched surface along with textured morphology contributed to the high contact angle. Janus PVDF membrane was therefore achieved via one single step unidirectional segregation strategy.

The thicknesses of hydrophilic layer and hydrophobic layer was determined by

dyeing the hydrophilic layer with congo red as exhibited in **Figure S7**. The water soluble congo red molecules intruded into the hydrophilic layer via the capillary effect and then repelled by the hydrophobic layer. A distinct red and blue layer was formed in the picture. It can be seen from **Figure S7** that the thickness for hydrophilic layer was 138.94 μm while the whole thickness of the membrane was 219.34 μm.

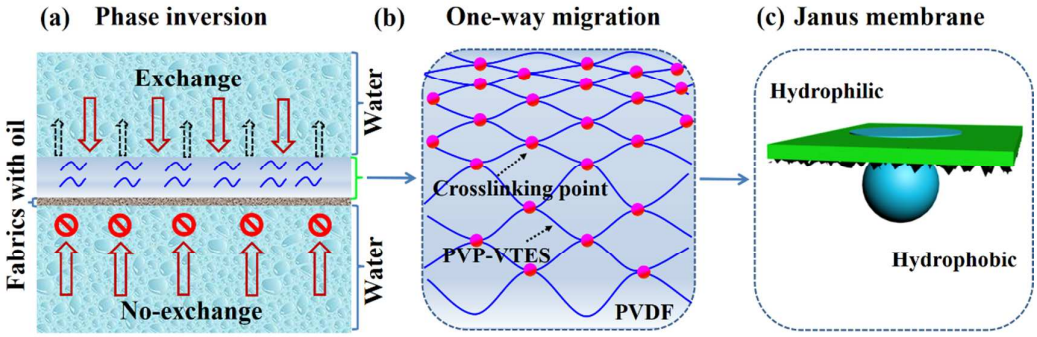

Figure 5. The fabrication of Janus membrane. (a) The presence of glycerol on non-woven fabric prevented the exchange of water/solvent on the bottom surface and exchange only occurred on the top surface. (b) PVP-VTES migrated to the top surface in a gradient way and anchored firmly as a network. (c) The top surface was hydrophilic and the bottom surface was hydrophobic.

3.4 Switchable emulsions separation

To investigate the peculiarity of Janus membrane in separating emulsions including oil-in-water emulsion and water-in-oil emulsion, the wettability and separation performances of hydrophobic membrane M1, Janus membrane M4 and hydrophilic membrane M5 were investigated. The underwater oil contact angles of top surfaces were illustrated in **Figure 6a**. M1 was hydrophobic with water contact angle 110^{o} for top surface in air. When it was immersed into water, the membrane can't be quickly wetted by water, resulting in the declined underwater oil contact angle (121^{o}). Therefore, the underwater oil contact angle for hydrophobic membrane M1 was the smallest among the three samples and there was no flux for M1 to separate oil-in-water emulsion as exhibited in **Figure 6c**. For M4 and M5, they all displayed underwater superoleophobicity as presented in **Figure 6a**, and the

oleophobicity of M4 with underwater oil contact angle 147° was better than that of M5 (138°) due to the enrichment of hydrophilic modifiers on top surface of M4.[31] It can be seen from Figure 6c that Janus membrane M4 exhibited better oil rejection over 97.5% separation efficiency compared with hydrophilic membrane M5. This can be explained from two aspects: M4 top surface possessed better hydrophilicity and underwater superoleophobicity and prevented oil from contacting and adsorbing to the membrane top surface; while the presence of hydrophobic bottom surface for Janus membrane increased the retention time of emulsion in membrane matrix, allowing small oil droplets to merge into bigger droplets[16], which is facilitated to the demulsification of entrapped emulsions.

For the bottom surface separation, it can be seen from **Figure 6b** that three samples presented underoil superhydrophobicity and M1 had higher underoil water contact angle (172°). For water-in-oil emulsion, the Janus membrane M4 exhibited similar separation performance with high efficiency and oil flux to M1 due to its underoil superhydrophobicity (170°) as exhibited in **Figure 6d**. M4 showed higher water-in-oil emulsion separation efficiency and oil flux compared with hydrophilic membrane M5 with underoil water contact angle 167°. Janus membrane M4 had higher underoil water contact angle due to few hydrophilic modifiers and more fluorine elements existing on bottom surface of M4 as exhibited in **Figure 4**, which was beneficial to high separation efficiency, and M5 was easily polluted by water droplets during separating water-in-oil emulsion, which would result in the declines of separation efficiency and oil flux. Therefore, it is quite simple to realize high efficient separation of both water oil-in-water and water-in-oil emulsions by turning over the Janus membrane.

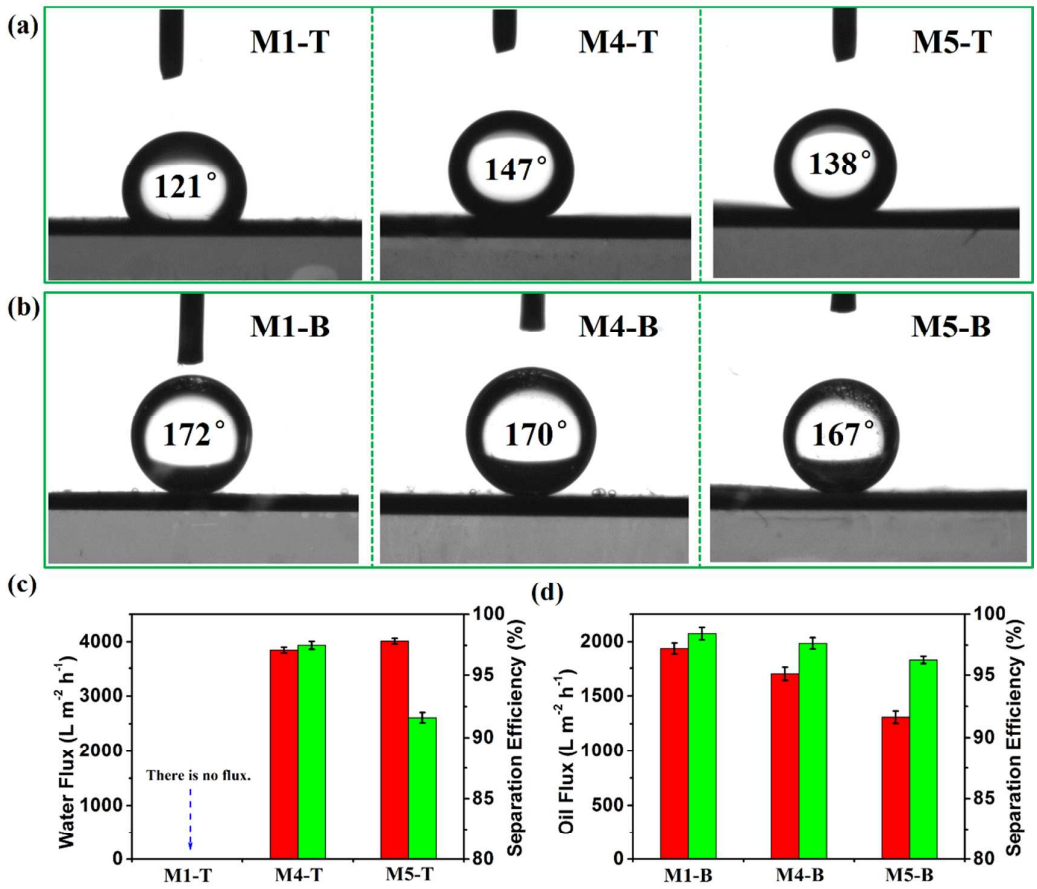

Figure 6. (a) The underwater oil contact angle of top surfaces for hydrophobic membrane M1, Janus membrane M4 and hydrophilic membrane M5 (oil: trichloromethane); (b) The underoil water contact angle of bottom surfaces (oil: toluene); (c) The water flux and separation efficiency for oil-in-water emulsion separation via top surface filtration; (d) The oil flux and separation efficiency for water-in-oil emulsion separation via bottom surface filtration.

4. Conclusion

In summary, Janus PVDF membrane was fabricated via single step unidirectional segregation strategy for the first time. The non-woven fabric was coated with oil to limit the exchange of water and solvent on the bottom surface during phase separation, and the hydrophilic copolymer PVP-VTES segregated to the top surface directionally driven by surface tension and then firmly anchored by the hydrothermal crosslinking. Working collaboratively with the asymmetric micro-/nano- structure caused by

non-woven fabric peeling, we achieved the final Janus membrane with extremely opposite wetting behavior, and the water contact angle difference ($\Delta\theta$) between top and bottom surfaces is up to 150^{o}, which is generally higher than previously reported results. The prepared Janus membrane exhibited switchable oil/water separation performance: it can separate oil-in-water emulsion with hydrophilic side and can also separate water-in-oil emulsion with hydrophobic side by simply turning over the membrane. In contrast, the hydrophobic membrane M1 was unable to separate oil-in-water emulsion, while the separation efficiency of hydrophilic membrane M5 was much lower than Janus membrane. The single step unidirectional segregation strategy simplify the Janus membrane preparation comparing to the previous post-modification and shows its potential application in membrane distillation, liquid/fog collection and liquid diode etc.

Acknowledgements

Financial support is acknowledged from National Key R&D Program of China (2017YFB0309604), National Nature Science Foundation of China (51603215, 5161101025), Youth Innovation Promotion Association of Chinese Academy of Science (2014258), Ningbo Science and Technology Bureau (2014B81004, 2017C110034).

Supporting Information

The word file contains additional contrast experiments and characterization of the thickness of hydrophilic layer. The Supporting Information is available free of charge on the ACS Publications website.

Notes

The authors declare no conflict of interest.

References

(1) De Gennes, P. G. Soft Matter. *Rev. Mod. Phys.* **1992**, 64, 645-648.

(2) Mihali, V.; Honciuc, A. Semiconductive Materials with Tunable Electrical Resistance and Surface Polarity Obtained by Asymmetric Functionalization of Janus Nanoparticles. *Adv. Mater. Interfaces* **2017**, 4, 1700914.

(3) Xie, Q.; Davies, G. B.; Harting, J. Direct Assembly of Magnetic Janus Particles at a Droplet Interface. *ACS Nano* **2017**, 11, 11232-11239.

(4) Wu, D.; Binks, B. P.; Honciuc, A. Modeling the Interfacial Energy of Surfactant-Free Amphiphilic Janus Nanoparticles from Phase Inversion in Pickering Emulsions. *Langmuir* **2018**, 34, 1225-1233.

(5) Luo, D.; Wang, F.; Vu, B. V.; Chen, J.; Bao, J.; Cai, D.; Willson, R. C.; Ren, Z. Synthesis of Graphene-Based Amphiphilic Janus Nanosheets via Manipulation of Hydrogen Bonding. *Carbon* **2018**, 126, 105-110.

(6) Meng, Q. B.; Yang, P.; Feng, T.; Ji, X.; Zhang, Q.; Liu, D.; Wu, S.; Liang, F.; Zheng, Z.; Song, X.-M. Phosphomolybdic Acid-Responsive Pickering Emulsions Stabilized by Ionic Liquid Functionalized Janus Nanosheets. *J. Colloid Inter. Sci.* **2017**, 507, 74-82.

(7) Ren, F.; Li, G.; Zhang, Z.; Zhang, X.; Fan, H.; Zhou, C.; Wang, Y.; Zhang, Y.; Wang, C.; Mu, K.; Su, Y.; Wu, D. A Single-Layer Janus Membrane with Dual Gradient Conical Micropore Arrays for Self-driving Fog Collection. *J. Mater. Chem. A* **2017**, 5, 18403-18408.

(8) Huang, Y.-X.; Wang, Z.; Jin, J.; Lin, S. Novel Janus Membrane for Membrane Distillation with Simultaneous Fouling and Wetting Resistance. *Environ. Sci. Technol.* **2017**, 51, 13304-13310.

(9) Wu, M. B.; Yang, H. C.; Wang, J. J.; Wu, G. P.; Xu, Z. K. Janus Membranes with Opposing Surface Wettability Enabling Oil-to-Water and Water-to-Oil Emulsification. *ACS Appl. Mater. Interfaces* **2017**, 9, 5062-5066.

(10) Yang, H. C.; Hou, J.; Chen, V.; Xu, Z. K. Janus Membranes: Exploring Duality for Advanced Separation. *Angew. Chem.* **2016**, 55, 13398-13407.

(11) Wang, Z.; Yang, X.; Cheng, Z.; Liu, Y.; Shao, L.; Jiang, L. Simply Realizing "Water Diode" Janus Membranes for Multifunctional Smart Applications. *Mater. Horiz.* **2017**, 4, 701-708.

(12) Yang, X.; Wang, Z.; Shao, L. Construction of Oil-Unidirectional Membrane for Integrated Oil Collection with Lossless Transportation and Oil-in-Water Emulsion Purification. *J. Membr. Sci.* **2018**, 549, 67-74.

(13) Wang, Z.; Wang, Y.; Liu, G. Rapid and Efficient Separation of Oil from Oil-in-Water Emulsions Using a Janus Cotton Fabric. *Angew. Chem.* **2016**, 55, 1291-1294.

(14) Wang, Z.; Liu, G.; Huang, S. In Situ Generated Janus Fabrics for the Rapid and Efficient Separation of Oil from Oil-in-Water Emulsions. *Angew. Chem.* **2016**, 55, 14610-14613.

(15) Wang, Z.; Lehtinen, M.; Liu, G. Universal Janus Filters for the Rapid Separation of Oil from Emulsions Stabilized by Ionic or Nonionic Surfactants. *Angew. Chem.* **2017**, 56, 12892-12897.

(16) Jiang, Y.; Hou, J.; Xu, J.; Shan, B. Switchable Oil/Water Separation with Efficient and Robust Janus Nanofiber Membranes. *Carbon* **2017**, 115, 477-485.

(17) Yang, H.-C.; Zhong, W.; Hou, J.; Chen, V.; Xu, Z.-K. Janus Hollow Fiber Membrane with a Mussel-Inspired Coating on the Lumen Surface for Direct Contact Membrane Distillation. *J. Membr. Sci.* **2017**, 523, 1-7.

(18) Yang, H.-C.; Hou, J.; Wan, L.-S.; Chen, V.; Xu, Z.-K. Janus Membranes with Asymmetric Wettability for Fine Bubble Aeration. *Adv. Mater. Interfaces* **2016**, 3, 1500774.

(19) Cao, M.; Xiao, J.; Yu, C.; Li, K.; Jiang, L. Hydrophobic/Hydrophilic Cooperative Janus System for Enhancement of Fog Collection. *Small* **2015**, 11, 4379-4384.

(20) Liu, Y.; Xin, J. H.; Choi, C.-H. Cotton Fabrics with Single-Faced Superhydrophobicity. *Langmuir* **2012**, 28, 17426-17434.

(21) Gu, J.; Xiao, P.; Chen, J.; Zhang, J.; Huang, Y.; Chen, T. Janus Polymer/Carbon Nanotube Hybrid Membranes for Oil/Water Separation. *ACS Appl. Mater. Interfaces* **2014**, 6, 16204-16209.

(22) Prince, J. A.; Rana, D.; Matsuura, T.; Ayyanar, N.; Shanmugasundaram, T. S.; Singh, G. Nanofiber Based Triple Layer Hydro-philic/-phobic Membrane - a Solution for Pore Wetting in Membrane Distillation. *Sci. Rep.* **2014**, 4, 6949.

(23) Wu, J.; Wang, N.; Wang, L.; Dong, H.; Zhao, Y.; Jiang, L. Unidirectional Water-Penetration Composite Fibrous Film via Electrospinning. *Soft Matter* **2012**, 8, 5996-5999.

(24) Essalhi, M.; Khayet, M. Surface Segregation of Fluorinated Modifying Macromolecule for Hydrophobic/Hydrophilic Membrane Preparation and Application in Air Gap and Direct Contact Membrane Distillation. *J. Membr. Sci.* **2012**, 417-418, 163-173.

(25) Zhang, Y.; Barboiu, M. Dynameric Asymmetric Membranes for Directional Water Transport. *Chem. Commun.* **2015**, 51, 15925-15927.

(26) Liu, F.; Hashim, N. A.; Liu, Y.; Abed, M. R. M.; Li, K. Progress in the Production and Modification of PVDF Membranes. *J. Membr. Sci.* 2011, 375, 1-27.

(27) Liu, Y.; Xin, J. H.; Choi, C. H. Cotton Fabrics with Single-Faced Superhydrophobicity. *Langmuir* **2012**, 28, 17426-17434.

(28) Hu, L.; Gao, S.; Zhu, Y.; Zhang, F.; Jiang, L.; Jin, J. An Ultrathin Bilayer Membrane with Asymmetric Wettability for Pressure Responsive Oil/Water Emulsion Separation. *J. Mater. Chem. A* **2015**, 3, 23477-23482.

(29) Bonyadi, S.; Chung, T. S. Flux Enhancement in Membrane Distillation by Fabrication of Dual Layer Hydrophilic–Hydrophobic Hollow Fiber Membranes. *J. Membr. Sci.* **2007**, 306, 134-146.

(30) Gao, X.; Zhou, J.; Du, R.; Xie, Z.; Deng, S.; Liu, R.; Liu, Z.; Zhang, J. Robust Superhydrophobic Foam: A Graphdiyne-Based Hierarchical Architecture for Oil/Water Separation. *Adv. Mater.* **2016**, 28, 168-173.

(31) Yang, H.-C.; Liao, K.-J.; Huang, H.; Wu, Q.-Y.; Wan, L.-S.; Xu, Z.-K. Mussel-Inspired Modification of a Polymer Membrane for Ultra-High Water Permeability and Oil-in-Water Emulsion Separation. *J. Mater. Chem. A* **2014**, 2, 10225-10230.

TOC:

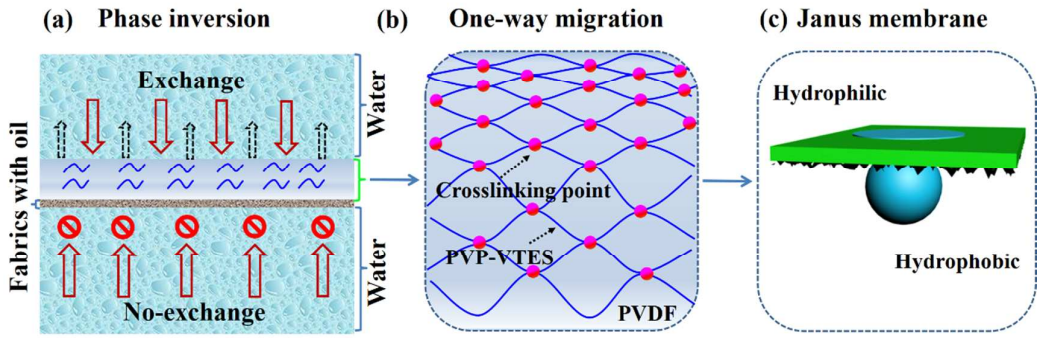
(a) Phase inversion
(b) One-way migration
(c) Janus membrane
Exchange
Water
Fabrics with oil
Water
No-exchange
Crosslinking point
PVP-VTES
PVDF
Hydrophilic
Hydrophobic